Am J Nucl Med Mol Imaging 2021;11(6):492-506
www.ajnmmi.us /ISSN:2160-8407/ajnmmi0138700

Original Article

Regional changes with global brain hypometabolism indicates a physiological triage phenomenon and can explain shared pathophysiological events in Alzheimer's & small vessel diseases and delirium

Sandeep K Gupta[1], Natalie Rutherford[1], Xenia Dolja-Gore[2], Tahne Watson[1], Balakrishnan R Nair[3]

[1]Department of Nuclear Medicine & PET, John Hunter and Calvary Mater Hospitals, Hunter Medical Research Institute (HMRI), University of Newcastle, Newcastle, NSW, Australia; [2]Research Centre for Generational Health and Ageing (RCGHA), Faculty of Health and Medicine, University of Newcastle, Newcastle, NSW, Australia; [3]School of Medicine and Public Health, University of Newcastle, Newcastle, NSW, Australia

Received August 29, 2021; Accepted October 9, 2021; Epub December 15, 2021; Published December 30, 2021

Abstract: While reduced global brain metabolism is known in aging, Alzheimer's disease (AD), small vessel disease (SVD) and delirium, explanation of regional brain metabolic (rBM) changes is a challenge. We hypothesized that this may be explained by "triage phenomenon", to preserve metabolic supply to vital brain areas. We studied changes in rBM in 69 patients with at least 5% decline in global brain metabolism during active lymphoma. There was significant decline in the rBM of the inferior parietal, precuneus, superior parietal, lateral occipital, primary visual cortices ($P<0.001$) and in the right lateral prefrontal cortex ($P=0.01$). Some areas showed no change; multiple areas had significantly increased rBM (e.g. medial prefrontal, anterior cingulate, pons, cerebellum and mesial temporal cortices; $P<0.001$). We conclude the existence of a physiological triage phenomenon and argue a new hypothetical model to explain the shared events in the pathophysiology of aging, AD, SVD and delirium.

Keywords: Alzheimer's disease, delirium, dementia, aging, small vessel disease, cerebral metabolism, cerebral perfusion

Introduction

While there are many similarities in radiological and pathological findings between normal aging, Alzheimer's disease (AD), cerebral small vessel disease (SVD) and delirium, no satisfactory pathophysiological explanation of a linkage is established [1]. Reduced global cerebral blood flow (gCBF) and global brain metabolism (gBM) is known in all these pathologies but only regional changes are observed in anatomical and functional imaging. Furthermore, a significant overlap of regional metabolic changes is observed. For example, while a typical pattern of perfusion/metabolic abnormalities is known with AD, similar changes are also seen in many non-AD disorders in the absence of amyloid beta (Aβ) and tau [2, 3] deposition and even in asymptomatic elderly persons [4-6]. For this reason, the recent National Institute of Aging and Alzheimer's Association (NIA-AA) research framework outlined that positive amyloid biomarkers are essential for AD diagnosis [6].

The brain is an extremely energy dependent organ and consumes 20% of overall metabolic requirement to function optimally [7, 8]. Consequently, even a small reduction in brain perfusion is of importance. In view of the adaptive nature of the brain [9], we hypothesized that a reduced brain metabolic supply may trigger a triage of available resources to preserve more vital areas for survival (e.g. autonomic, motor and brain stem function). Other domains such as cognitive function, may be of low priority when survival is the only aim.

It would be unethical to create an artificial reduction in gCBF/gBM in humans. Henceforth, we captured another common scenario to preliminarily study this hypothesis. FDG PET/CT brain in severe lymphoma may demonstrate reduced gBM, which is near completely revers-

ible after chemotherapy. In this study, we aimed to evaluate variations in regional brain metabolism (rBM) when gBM is reduced (pre-therapy PET) versus when gBM is normal/near normal (post therapy PET).

Material and methods

Patient selection

Thirty thousand, seven hundred and thirty one 18F-FDG PET/CT scans were performed in the Department of Nuclear Medicine & PET in our institution between Jan 2010, and Jan 2020. 1,513 PET scans performed for initial staging of lymphoma were retrospectively reviewed by a nuclear medicine physician (SG) with 13 years' PET experience. 75 patients satisfying all the following criteria were selected-large volume disease on pre therapy PET on visual assessment of MIP imaging, nil brain metastases or CNS lymphoma, availability of a post therapy PET demonstrating either complete or near complete metabolic response, all PET acquisition with arms by patient's side, nil head motion between CT and PET, absence of any unwarranted systemic FDG activities (e.g. pleurodesis, significant extravasation of injected dose, significant brown fat or muscular activities etc.), BGL <8.0 mmol/L and lack of significant marrow activity in the post therapy PET. One patient was later excluded due to a small occipital infarct in the post therapy PET. The remaining 74 scans were further reviewed and confirmed eligible by another nuclear medicine physician (NR) with 14 years of experience in PET scans. After quantitative analysis (as described below), five patients with <5% decline in gBM were excluded since the study aim was to test regional changes "only when there is decline in gBM". The hospital records and routine pre-imaging patient questionnaire of the study patients were reviewed to document vascular risk factors e.g. smoking, hypertension, obesity, diabetes mellitus and prior stroke. This retrospective study was approved by the local research ethics committee.

FDG PET acquisition and image analysis

FDG PET studies were performed using a GE 870 PET/CT digital scanner with 1.5 min per bed position and Q.Clear reconstruction algorithm with a beta value (optimum penalization factor) of 550. Prior to June 2018, the studies were obtained on GE Discovery-690 3D PET/CT scanner (General Electric Medical Systems, Milwaukee, Wisconsin, USA) with 2.0 min per bed position and time-of-flight reconstruction algorithm. The CT was performed using a pitch of 0.984, 120 kV, automA with a noise index of 42. The scans are performed 60 minutes after administration of weight adjusted (2.5 MBq/kg) intravenous 18FDG after a minimum of four hours' fasting. The images were displayed on an Advanced Workstation (AW version 3.3 Ext 1.2; GE healthcare, Milwaukee, Wisconsin, USA). All the SUV calculations were as a default, corrected for lean body mass. Following image analyses were performed on all 69 paired PET scans by a single investigator (SG).

gBM: Using the semiautomated PET VCAR software (AW workstation-GE healthcare), a 3D ROI was placed around the brain. Rarely non-brain very close by FDG activities (e.g. related to orbital muscles, skull marrow, neck muscles or nodes) were included in the automated contouring giving an overestimation of metabolic volume. These, if present, were manually excluded from the contouring to provide accurate brain metabolism. gBM was represented by total brain metabolic volume multiplied by total brain SUVmean and was automatically calculated by the software.

Manual rBM assessment: The transaxial attenuation corrected PET images were displayed and absolute rBM was assessed by measuring SUVmax. This data was collected using a minimum of 96 mm^2 2D ROI was placed at various parts of the brain (frontal and parietal grey matter, frontal and parietal white matter, basal ganglia, thalami, and cerebellum bilaterally).

Automated relative rBM assessment: Using a dedicated, completely automated software (CortexID Suit, Version 2.1 Ext. 6, GE healthcare - General Electric Medical Systems, Milwaukee, Wisconsin, USA), the uptake ratio values (normalized to global brain) of the various brain areas were tabulated for each PET scan. Global normalization is used instead of pons or cerebellum as we did expect regional metabolic changes in the latter areas.

Statistical analysis

Statistical analysis was conducted using JMP Pro 14.2.0 (SAS Institute). Shapiro-Wilk W Test

Table 1. Patient characteristics

Patient Characteristic N=69	% (N)
Gender	
Male	52.2% (36)
Female	47.8% (33)
Total number of vascular risk factors	
No known risk factors	47.8% (33)
One risk factor	30.4% (21)
Two risk factors	17.4% (12)
Three risk factors	2.9% (2)
Four risk factors	1.4% (1)
Vascular risk factors	
Hypertension	33.3% (23)
Dyslipidaemia	14.5% (10)
Ischaemic Heart Disease	10.1 (7)
Diabetes	5.8% (4)
Others*	15.9% (11)
Type of Lymphoma	
Diffuse large B cell lymphoma (DLBCL)	72.5% (50)
Follicular	7.2% (5)
Hodgkin's	5.8% (4)
Mantle cell	4.3% (3)
Others	10.1% (7)
Therapy received	
R-CHOP	72.5% (50)
Other	27.5% (19)
	Mean (std)
Age (years)	64 (16)
Age of females	66 (15)
Age of males	61 (17)
Duration between the two PET scans (months)	5.8 (2.3)
Injected FDG dose (MBq)	
Pre-therapy	211 (31)
Post-therapy	210 (29)
Blood Glucose Level (mmol/L)	
Pre-therapy	5.3 (0.9)
Post-therapy	5.2 (0.7)
Patient weight (kg)	
Pre-therapy	75.0 (17.2)
Post-therapy	74.1 (16.6)

*Peripheral vascular disease, Cerebrovascular disease, Smoker, Obesity, Chronic renal failure.

identifies almost all individual readings as normally distributed although some minor variations are noted. In these cases, normal quantile plots were used to assess their acceptability for further inclusion. Differences display a similarly normal profile in the absence of outliers. Paired t-tests were used to compare differences pre-post and left-right. Simple linear regression models were performed to identify significant differences between brain regions and multivariate linear regression models performed using the independent variables while accounting for total glycolytic volume. Bland-Altman was used to assess inter-rater agreement. For all statistical analyses $P<0.05$ is considered as a statistically significant difference, while $P<0.001$ is taken as a highly significant difference.

Correlation between the two observers in sixteen studies of eight patients was extremely high (>0.99). Bland-Altman test identifies a minor bias between readers (114.9±803.1) but no significant difference ($P<0.001$).

Results

The study comprised of 69 patients with mean age 64±16 years and with an almost equal gender distribution (48% females vs 52% males) (**Table 1**). Patient vascular risk factor counts ranged from 47.8% with zero, 30.4% with one, 17.4% with two and 4.3% with less than five. Hypertension was the most common vascular risk factor (33.3%). A majority of patients had diffuse large B cell lymphoma (72.5%) and a majority had received R-CHOP therapy (72.5%) with occasional minor variations. No difference in the FDG dose, blood glucose level or weight was observed between the paired pre- and post-therapy PET scans (**Table 1**).

With active lymphoma pathology, there was a mean 40.7% (range 6.0% to 85.1%) decline in the gBM compared to normal post therapy state ($P<0.001$). During brain hypometabolism, all the assessed brain regions had marked decline in absolute metabolism as assessed by SUVmax (**Figure 1**). The mean percentage decline was maximal in frontal and parietal cortices (42.8%-45.3%), followed by thalami and basal ganglia (40.7%-41.7%) and cerebellum (left =36.8%, right =37.9%). The mean decline in white matter in parietal and frontal regions was relatively less (31.7%-33.3%). All these reductions were highly significant ($P<0.001$).

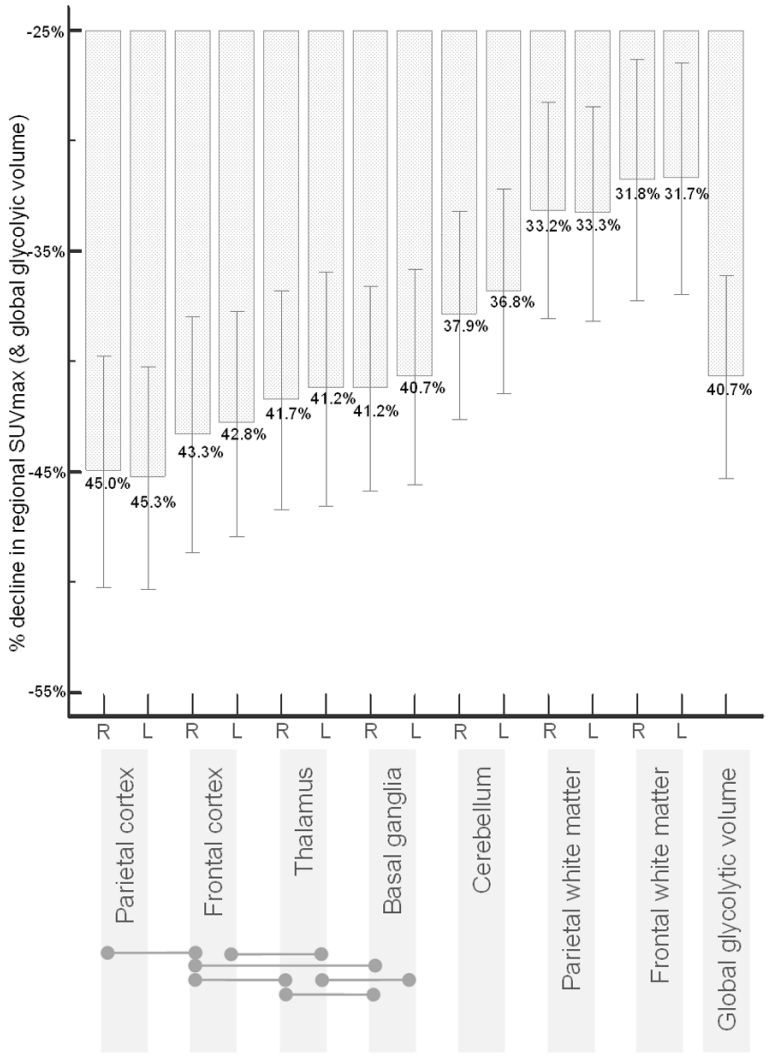

Figure 1. Relative % reduction in SUVmax in some cortical and subcortical regions with global hypometabolism (as measured manually by drawing region of interests). % reduction in global hypometabolism is on the far-right column for reference only. For each area, R= right & L= left hemisphere, as depicted on x-axis. Each bar represents mean % decline; 95% CI of mean is also shown with solid lines. Paired analysis between the individual regions of the same hemisphere (except white matter) was performed to assess difference. A total of ten pair combinations in each hemisphere were possible. The relative decline in all the areas is significantly different to others except four regions "bilaterally" (P>0.05). These non-significantly different combination pairs are shown in light green horizontal bars at the bottom of the image.

When 'relative' decline of each area (excluding white matter) is compared to the remainder of the areas in the same cerebral hemisphere, a total of twenty such paired combinations in each hemisphere were possible. Metabolic decline in all, except six, combination locations were statistically different, indicative of regional variations in metabolism. For example, percentage decline in SUVmax in the right parietal cortex was significantly significant relative to the ipsilateral thalamus (P=0.001), basal ganglia (P<0.001), and cerebellum (P<0.001), but not from the frontal cortex (P= 0.05) (**Figure 1**).

Quantitative automated detailed analyses of relative metabolism, using CortexID software, showed that with reduced gBM, there was a significant percentage decline in the rBM of the inferior parietal, precuneus, superior parietal, lateral occipital, and primary visual cortices (P< 0.001) as well as in the right lateral prefrontal cortex (P= 0.01) (**Figure 2**). While many regional areas showed no change (e.g. bilateral posterior cingulate, sensory-motor, lateral temporal as well as left lateral prefrontal cortices), multiple areas had significantly increased rBM (e.g. medial prefrontal, anterior cingulate, pons, cerebellum and mesial temporal cortices; P<0.001). Mean maximum decline in rBM was 10.0% in the right primary visual cortex and mean maximum increase was 12% in the left mesial temporal cortex (**Table 2**).

To assess the effect of increasing severity of gBM decline, we attempted to replicate the analyses in stepwise 20% decline in gBM. However, the sample size of patients with >20% decline in gBM was too large (n=60), similar to overall study patients. Patient numbers with >60% decline in gBM was considered too small (n=12). A reduction of greater than 40% cut off was selected giving a reasonable sample size (n=31). In quantitative analyses of the latter subgroup, the percentage changes in rBM were much more marked and the mean values ranged from -15.4% to +18.5%. Only right posterior cingulate

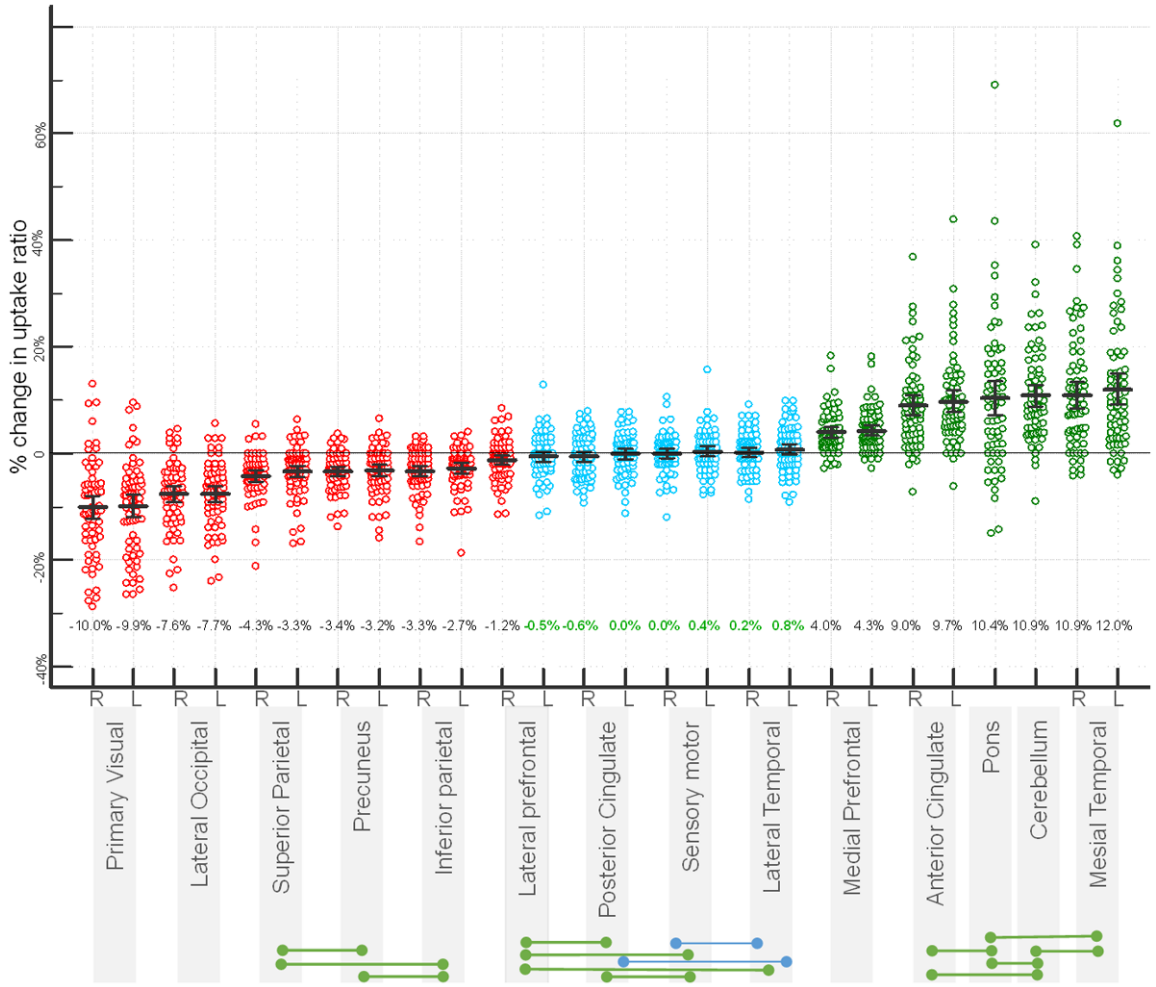

Figure 2. Relative % regional metabolic changes in various grey matter areas with global hypometabolism (as measured by automated uptake scores using CortexID software). All patients (n=69) values are shown by coloured circles and mean +95% CI is shown by black solid bars. X-axis denotes areas (in ascending mean % changes) and Y-axis denotes % changes (increase or decrease). The areas with statistically significant decline are shown in red, significant increase are shown with green whereas nonsignificant (P>0.05) change is shown with blue circles. Paired analyses of all the individual areas compared all the other areas in the same hemisphere were performed, which showed no significant differences between the paired areas depicted at the bottom of the image with solid horizontal bars. The green bars indicate no differences in both hemispheric regions whereas blue bars indicate no statistical differences only in unilateral hemisphere pair combination. Pons and cerebellum had a single value. Difference between all the other pair combinations was statistically significant. (In automated analyses, cerebellum and pons are analysed as a single region rather than right or left).

cortices (2.1% decrease) and left sensorimotor cortices (2.0% increase), which were unchanged in all patient analyses, were then found to be significantly different in subgroup analyses of >40% decline in gBM. Otherwise, paired analyses were of similar pattern, but the regional changes were more pronounced (**Table 2**).

Uptake ratio in each area during decline in gBM was compared to all the other areas in the same hemisphere. There were a total of 181 possible pairs. Changes in all except 24 pair combination values, as shown in **Figure 2**, were statistically different. This finding is further consistent with rBM variations.

When global hypometabolism-induced relative changes in right and left hemispheric areas were compared, only lateral prefrontal (mean change left -0.5%, right -1.2%; P=0.025) and sensorimotor (mean change left side 0.4%, right side 0.0% P=0.024) had mild differenc-

Table 2. % change in regional metabolism (uptake score) when there is global hypometabolism

Region	% Change (CI%)-All patient (n=69)	*P*-value	% Change in subgroup of >40% decline in gBM (n=31)
Primary Visual (R)	-10.0% [(-12.2%)-(-7.9%)]	<0.001	-15.4% (P<0.001)
Primary Visual (L)	-9.9% [(-11.9%)-(-7.8%)]	<0.001	-14.8% (P<0.001)
Occipital Lateral (L)	-7.7% [(-9.1%)-(-6.2%)]	<0.001	-10.4% (P<0.001)
Occipital Lateral (R)	-7.6% [(-9.1%)-(-6.1%)]	<0.001	-10.5% (P<0.001)
Parietal Superior (R)	-4.3% [(-5.3%)-(-3.2%)]	<0.001	-4.9% (P<0.001)
Precuneus (R)	-3.4% [(-4.2%)-(-2.5%)]	<0.001	-4.9% (P<0.001)
Parietal Superior (L)	-3.3% [(-4.4%)-(-2.2%)]	<0.001	-2.9% (P=0.003)
Parietal Inferior (R)	-3.3% [(-4.2%)-(-2.3%)]	<0.001	-4.7% (P<0.001)
Precuneus (L)	-3.2% [(-4.3%)-(-2.2%)]	<0.001	-4.8% (P<0.001)
Parietal Inferior (L)	-2.7% [(-3.7%)-(-1.8%)]	<0.001	-3.3% (P<0.001)
Prefrontal Lateral (R)	-1.2% [(-2.2%)-(-0.3%)]	0.01	-2.1% (P=0.006)
Posterior Cingulate (R)	-0.6% [(-1.5%)-(0.4%)]	0.26*	-2.1% (P=0.004)
Prefrontal Lateral (L)	-0.5% [(-1.5%)-(0.4%)]	0.26*	-1.3% (P=0.06)*
Posterior Cingulate (L)	0.0% [(-1.0%)-(0.9%)]	0.94*	-1.0% (P=0.11)*
Sensorimotor (R)	0.0% [(-0.92%)-(0.9%)]	0.95*	0.4% (P=0.62)*
Temporal Lateral (R)	0.2% [(-0.7%)-(1.1%)]	0.66*	-0.2% (P=0.71)*
Sensorimotor (L)	0.4% [(-0.5%)-(1.4%)]	0.36*	2.0% (P=0.01)
Temporal Lateral (L)	0.8% [(-0.2%)-(1.78%)]	0.13*	0.5% (P=0.57)*
Prefrontal Medial (R)	4.0% [(3.0%)-(5.0%)]	<0.001	5.2% (P<0.001)
Prefrontal Medial (L)	4.3% [(3.4%)-(5.3%)]	<0.001	5.6% (P<0.001)
Anterior Cingulate (R)	9.0% [(7.2%)-(10.9%)]	<0.001	13.1% (P<0.001)
Anterior Cingulate (L)	9.7% [(7.7%)-(11.7%)]	<0.001	14.2% (P<0.001)
Pons	10.4% [(7.2%)-(13.6%)]	<0.001	16.4% (P<0.001)
Cerebellum Whole	10.9% [(8.8%)-(13.0%)]	<0.001	15.2% (P<0.001)
Temporal Mesial (R)	10.9% [(8.5%)-(13.4%)]	<0.001	16.9% (P<0.001)
Temporal Mesial (L)	12.0% [(9.2%)-(14.9%)]	<0.001	18.5% (P<0.001)

*P>0.05 (non-significant).

es. These were considered non-specific and were likely due to physiological hemispheric dominance.

Using all 69 patients, the explanatory variables age, sex and number of vascular comorbidities were regressed against each significant brain region (as shown in **Figure 2**) in turn while controlling for gBM. A gender differential was noted (**Figure 3**) with females displaying an increase in rBM for Right Anterior Cingulate (1.64% P=0.03) and Right Temporal Mesial (1.93% P=0.04) but a decrease for Superior Parietal (left, right: -1.26% P=0.03, -1.23% P=0.008, respectively), Primary Visual (left, right: -2.63% P<0.01, -2.20% P<0.01, respectively) and right lateral occipital (-1.45% P=0.02).

Only one area significantly varied with vascular risk factors when controlled for gBM (left lateral occipital cortex, 1.32% P=0.048). Only three areas (right medial prefrontal, left superior parietal and pons: 0.07% P 0.01, -0.08% P 0.03 and -0.18% P 0.04 respectively) varied significantly with age. In view of only isolated and/or small differences, in the authors' opinion, aging and vascular risk factors do not influence triage to any clinical relevance.

FDG PET images of a study patient have been summarised in **Figure 4**.

Discussion

The study aimed to evaluate our hypothesis that with a reduction in gBM, changes occur in rBM indicative of a triage phenomenon. Sixty-nine patients with more than 5% decline in gBM during active lymphoma (relative to post therapy) were evaluated. During reduced gBM, all the regional brain areas had reduced 'absolute' metabolism. However, between

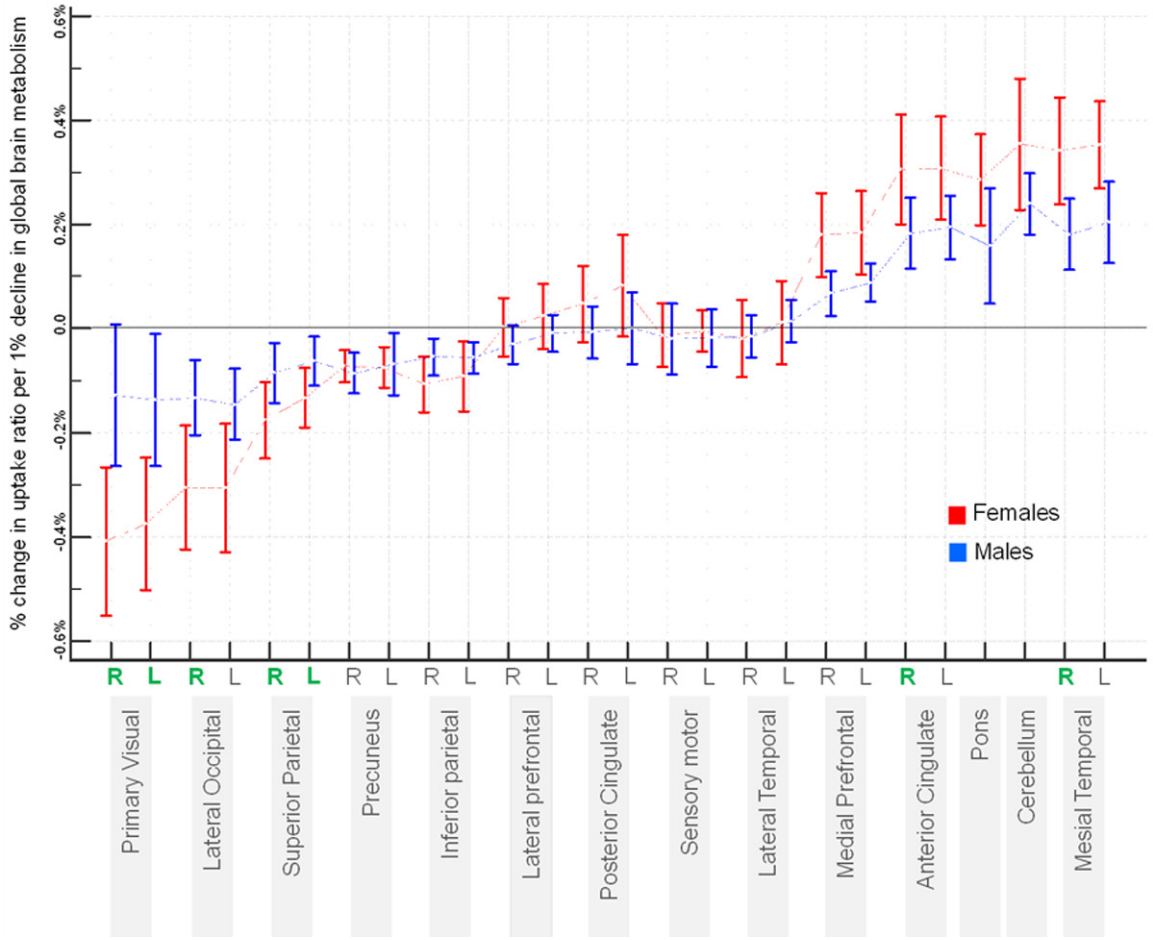

Figure 3. Male versus female changes in rBM per 1% drop in gBM. Mean values are shown by dotted lines and 95% CI of mean by solid bars for males (blue bars) and females (pink bars). Note that females have relative more metabolic decline in regions mentioned in left side of the figure as well as more metabolic increase in regions mentioned in right side of the figure. This indicates more pronounced triage phenomenon in females compared to males when there is similar degree of reduction in gBM. The statistically significant regions are highlighted with green font. (In automated analyses, cerebellum and pons are analysed as a single region rather than right or left).

regions, there was a distinct pattern of metabolic changes. Reduced rBM was found in primary visual, lateral occipital, superior and inferior parietal, precuneus as well as right lateral frontal cortices, whereas increased rBM was demonstrated in mesial temporal, cerebellum, pons, anterior cingulate and medial prefrontal cortices. Explicably, former areas are the low priority areas whereas latter are likely more vital for survival. This triage phenomenon was significantly more pronounced in many areas in females, compared to males. In light of this crucial physiological information, we propose a new hypothetical model outlining the pathophysiological process and interactions of the common cognitive pathologies (**Figures 5**, **6**).

Firstly, the aetiology of reduced gBM on FDG PET requires elucidation. Reduced gBM is a well-known occurrence with lymphoma, chemotherapy, drug induced marrow reactivation (e.g. erythropoiesis and colony stimulating factors) as well as infective and non-infective inflammatory pathologies [10-16]. One plausible explanation may be a physiological diversion of radio-glucose towards a high volume inflammatory or malignant process. Thence less injected FDG activity is available for brain but in our experience, reduced gBM is also seen in small volume malignancies. A second, more likely explanation may be blood brain barrier (BBB) dysfunction. Glucose transporter 1 (GLUT-1) is expressed in the microvascular endothelial cells of the BBB and glia, whereas GLUT-3 is

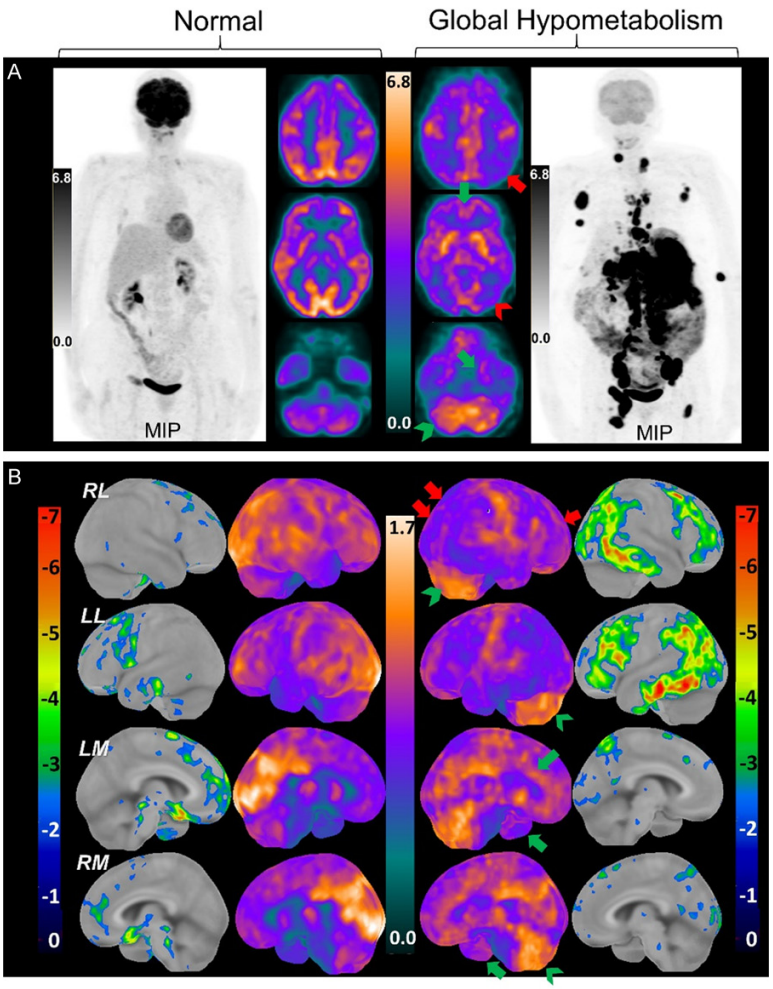

Figure 4. FDG PET images of a 73-year old female with DLBCL. The left two columns represent images with normal brain metabolism and images when global hypometabolism are shown in right two columns. The two imaging are five months apart. A. Only minor changes in MIP imaging (1st column) and three axial brain slices (2nd column). However with a 67.7% reduction in total brain metabolism with lymphoma (MIP image 4th column), matched axial slices show reduced rBM in parietal (red arrow) & parieto-occipital (red arrow head) cortices whereas increased metabolism in anterior cingulate & mesial temporal cortices (green arrow) and cerebellum (green arrow head). B. The Stereotactic Surface Projection- Uptake Ratio images are shown in 1st and 4th column and Uptake Ratio MIP images generated by cortex ID software (normalized to global brain) are shown in 2nd and 3rd columns. RL- Right lateral; RM- Right medial; LL: Left lateral; LM: Left medial. The reduced metabolic areas are shown with red arrows and increased metabolic areas are shown with green arrows and arrow heads.

expressed in neurons [17]. FDG entry to the brain is facilitated by GLUT-1 receptors [18]. Hence, reduced gBM could result from either BBB or neuronal injury. Later is unlikely in view of reversibility after correction of illness. Of note, the cerebral perfusion and metabolism are highly coupled, [19-22] even in persistent vegetative state [23]. BBB dysfunction, alone, cannot explain the degree of reduced gBM in our study patients. For example, up to 45% to 58% decline in perfusion and metabolism is seen in minimally conscious or vegetative patients [23, 24]. Thus, in view of a severe (up to maximum 85.5%) decline in gBM, we believe that reduced gBM in our patients is most likely indicative of ischemic BBB injury; and is in part contributed by radioglucose diversion to highly metabolic extracranial lesions.

Secondly, we outline the fact that reduced gCBF/gBM is well known to be associated with physiological aging [25-27], sickness behaviour [28], hyperthermia [25], delirium [9, 29-33], malignancy, chemotherapy, acute or chronic inflammation (either infective or non-infective) [10-16], anaesthesia [34-37] as well as AD [22, 38-43]. For example, anaesthesia leads to 26.8% decrease in gCBF in the sedated state [35] and 27.6% to 54.4% reduction in the anesthetized state [35-37]. A combination of latter with aging and surgery related inflammation, may result in more severe decline in gBM leading to higher probability of delirium perioperatively [44, 45]. Predictably, during delirium, a mean 42.2% decline in gCBF is demonstrated [30]. This explains delirium related ischaemic changes on radiological (white matter hyperintensities, lower brain volume, atrophy and infarcts), biochemical (elevated CSF lactate and pyruvate) as well as pathological (hypoxic vascular damage leading to impaired BBB function) investigations [9, 33, 46] despite nil acute brain involvement by disease [40, 47]. Reduction in gCBF in AD is also well known, related to amyloid toxicity [48, 49]. Since in all the above mentioned conditions, reduced gBM likely reflects BBB injury,

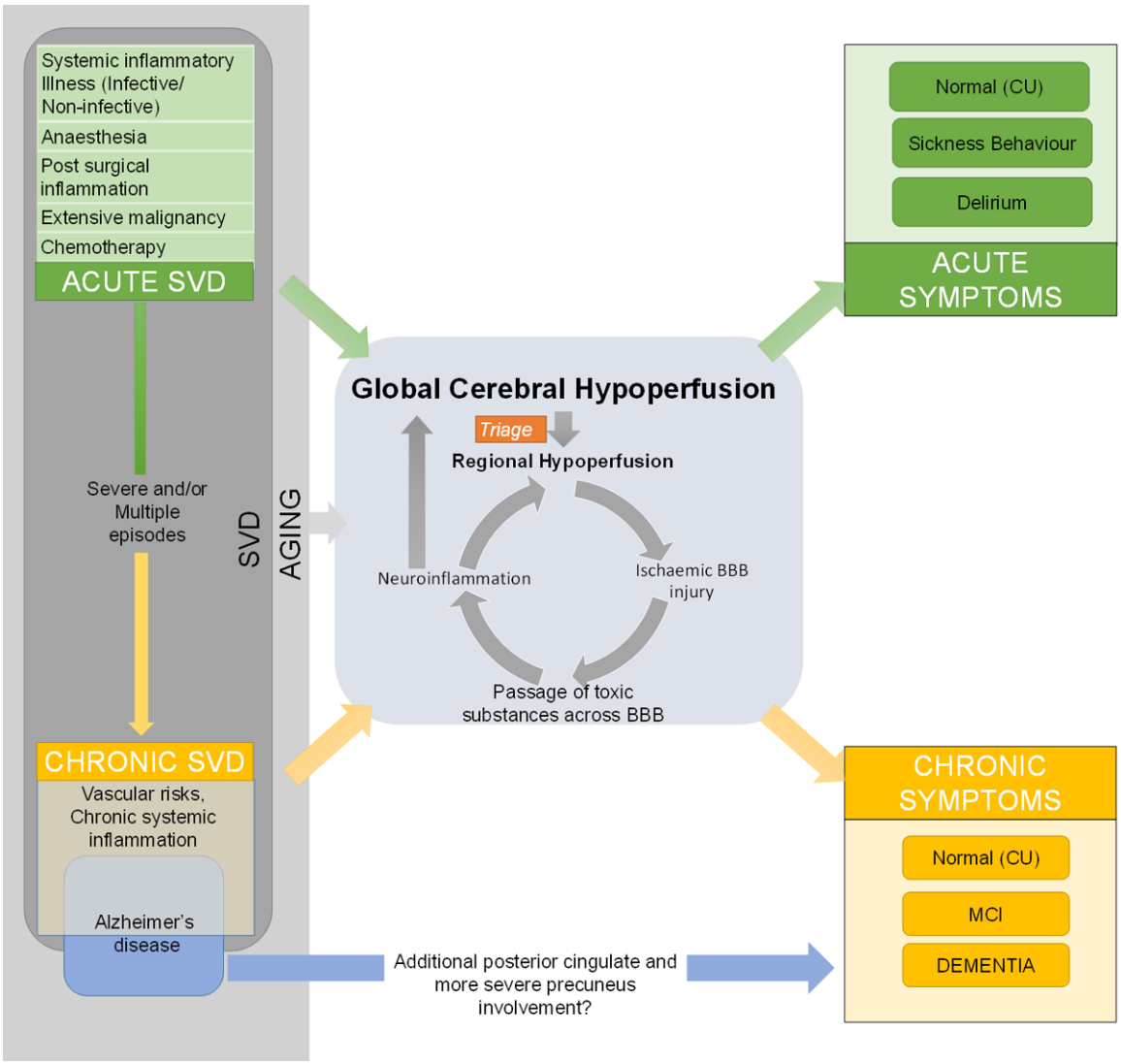

Figure 5. Hypothetical model of pathophysiological interaction between the acute and chronic pathologies on brain perfusion and clinical outcome. Aging is the most important template for all the diseases but SVD is the second largest contributor. SVD can be due to acute or chronic illnesses (including partly AD). While acute illness are potentially reversible, some residual deficits contribute to chronic illnesses especially when multiple episodes. Chronic SVD is not only from vascular risk factors but also from AD. Hence a majority of perfusion/metabolic abnormalities in AD perhaps due to secondary to that of SVD but additional deficits e.g. posterior cingulate and more severe precuneus involvement is likely unrelated to SVD pattern. All these illnesses lead to global cerebral hypoperfusion/hypometabolism and due to triage, there is relatively more ischemic BBB injury, neuroinflammation leading to a vicious cycle whereby more toxic systemic materials can penetrate the brain. The outcome can be acute whereby depending on severity of disease and age, this may be asymptomatic (Cognitively unimpaired CU) or may lead to sickness behaviour or delirium. Chronic outcomes may be either asymptomatic or minimal cognitive impairment or dementia.

we believe these conditions may be classed as non-thromboembolic, cerebral SVD (**Figure 5**).

Thirdly, a large amount of literature shows reduced gBM and consequent variations in rBM, further supporting the triage phenomenon. In vegetative patients, 58% decline in gBM led to 62% decline in precuneus but only 35% decline in brainstem metabolism [24]. Similar changes in rBM or rCBF have been demonstrated with systemic inflammation in animal studies [50], sickness behaviour [47, 50] and even with physiological aging [49, 51, 52]. A reduced gBM/gCBF may lead to ischemic BBB injury in predominantly low priority brain regions. Subsequently, via a cascade of events, neuroinflammation results, which is further exacerbated by passage of vasculotoxic and neurotoxic

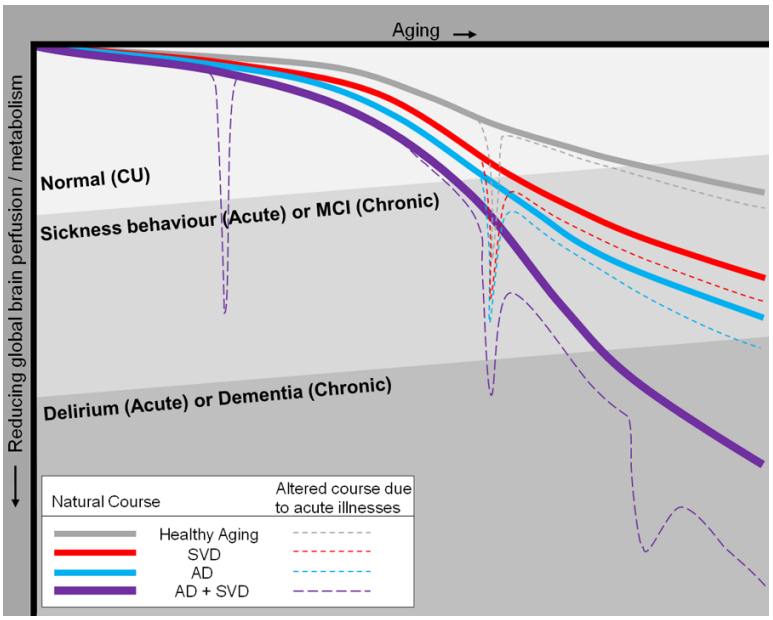

Figure 6. Hypothetical model of relationship of cerebral perfusion/metabolism and natural course in acute and chronic conditions. The x-axis represents increasing age and y-axis represents declining global cerebral perfusion/metabolism (not to scale). Firstly, healthy aging (solid grey line) leads to progressive reduction in brain perfusion/metabolic changes, but these are more pronounced with AD (AD-solid red line), SVD (SVD-solid blue line) and even more pronounced with both AD + SVD (solid purple line). With all conditions, decline in perfusion is slow in early age but is more rapid in middle age onwards. Secondly, each episode of acute pathology (as shown with dotted line spikes) alters the natural course of disease to worsening as shown by dotted lines of respective colours. In younger age, acute illness has only minimal or nil longer-term consequences but middle age onwards each episode is associated with more residual perfusion deficit as shown with altered natural course shown by dotted lines. Thirdly, in younger age, recovery from even a severe acute illness is quicker, but with advancing age, the recovery is slower even with mild acute illness (as shown by widening of spikes). Finally, threshold for symptoms varies with aging. Small decline in brain perfusion is asymptomatic but more severe decline can lead to sickness behaviour (or mild cognitive decline if chronic) or delirium (or dementia if chronic). The symptoms vary with patients' cognitive reserve, age, genetic profile and co-morbidities e.g. vascular pathologies, anaemia, hypoxia etc.

substances across the BBB [18, 21, 22, 28, 40, 41, 53-55] (**Figure 5**). Expectedly, multiple studies have demonstrated temporoparietal, frontal and occipital hypoperfusion in delirium patients [9, 29, 31, 45, 47].

While acute SVD may be completely reversible when precipitating illness resolves, this ischemic event may lead to at least some degree of residual irreversible chronic neuronal injury particularly with severe illness, multiple risks and with aging [1, 9, 33, 47, 56]. Chronic conditions (e.g. aging, vascular risk factors or chronic inflammation related) with resultant chronic SVD likely leads to chronic, slowly worsening changes. This is substantiated by a recent study by Di et al [57] who followed healthy individuals yearly with FDG PET for five years and demonstrated age related reduction in rBM in visual cortex, posterior parietal cortex, anterior temporal, insular, orbitofrontal and cingulate cortices. They found increased rBM in cerebellum, basal ganglia, insula, amygdala, thalami and sensory motor cortices [57]. Our study shows a close pattern of regional metabolic changes further supporting our hypothesis.

Symptomatically, acute SVD can lead to either no cognitive changes or sickness behaviour or delirium. Younger age and high cognitive reserve (highly connected brain and preserved plasticity) are protective factors [58]. Sickness behaviour is a spectrum of metabolic and behavioural changes to conserve energy and maximize the probability of recovery [9, 59, 60]. Exemplifying this, similar illness at a young age may lead to either no symptoms or sickness behaviour but in vulnerable brain (e.g. aging, pre-existing cognitive impairment or co-existing brain pathologies) this can cause delirium [9, 33, 41, 47]. Similarly, chronic SVD may lead to nil cognitive changes or minimal cognitive impairment or dementia depending on severity of illness and cognitive reserve of an individual [61, 62].

Here we emphasize the known fact that the most important and crucial substrate for many brain pathologies is aging [53]. Aging brain cannot withstand the metabolic stress in the same way as young healthy individuals and becomes increasingly vulnerable to hypoxic stress resulting from a variety of pathophysiological changes [42, 46, 53]. With aging, the gCBF declines by approximately 2.7 to 4.8 mL/min per year

[25-27] after 5-6 years age and exponentially among the elderly (9.38 mL/min per year) [26]. Interestingly, while brain aging is assumed to be linear in trend, fluctuations are seen along this trend [57] which may be explained by intermittent episodic illnesses (**Figures 5**, **6**).

Fourthly, the predominant pathophysiological abnormality in AD is diffuse high Aβ deposition [18, 40, 63-67]. Our triage hypothesis explains a well-known dilemma of only rBM changes on FDG PET despite Aβ found diffusely throughout the neocortex [68-70]. In AD, while a reduced rBM on FDG PET is seen in the parieto-temporal association area, posterior cingulate, precuneus and frontal association areas [2, 4, 21, 64], increased rBM is demonstrated in sensory motor cortices, thalami, pons, cerebellum and anterior cingulate cortices [71]. While we can explain a majority the changes by our triage hypothesis (similar to SVD), posterior cingulate and more pronounced precuneus abnormalities are the deviations. Hence, we believe that while AD is predominantly a subset of chronic SVD, above discrepant finding in these two areas argues for additional pathophysiological mechanism requiring further studies.

An interesting finding in our study was the sex difference in triage. Females have approximately 12.1% higher mean gCBF than men [25, 72] but still have higher incidence of AD and worse cognitive functions when suffering from AD [7]. Findings from the European Studies of Dementia (EURODEM) network show a 54% higher relative risk of AD for females, adjusting for age and education compared to males [73]. Almost two-thirds of Americans with AD are females and estimated lifetime risk for AD at age 45 is twice that of men [74]. We believe significantly more pronounced triage related metabolic changes in females can explain this (**Figure 3**).

Another interesting finding is a more pronounced triage related reduction in occipital rBM. In a study by Chiotis et al., increased THK5317 tau binding in occipital lobe in AD was associated with cognitive impairment despite FDG PET showing no significant difference [75]. Recently, Huang et al. compared 50 AD patients with 30 controls and showed 14.2% decline in gCBF in AD with maximum reduction in perfusion in the occipital cortices (22.3%) followed by parietal (18%), lateral temporal (13.3%) and frontal (12.0%) cortices [28]. Furthermore, occipital hypometabolism has been demonstrated during delirium episodes [33]. Hence, we believe occipital lobe is truly involved in any SVD related conditions, but this is not manifested early due to relative high reserve and greater physiological variations.

We found increased rBM in mesial temporal cortices with triage arguing its importance in survival. No surprisingly, this area regulates enhanced memory for stimuli that are of adaptive importance to survival [76]. This finding is further substantiated by a recent study by Huang et al. showing a 14.2% decline in gCBF in AD is associated with least reduction in perfusion in medial temporal cortex (9.1%) relative to occipital (21.3%), parietal (18%), lateral temporal (13.3%) and frontal (11.9%) cortices [28].

Similarly, relative increased rBM in anterior cingulate cortex (ACC) indicates its value for survival. ACC is known as a “neural alarm” that serves to direct attention toward potential conflicts with enduring survival goals [77]. A substantial body of evidence also implicates ACC dysfunction in depression [77-79] and depressed suicides [80]. Therefore, during an illness, relative preservation of rBM is probably an evolutionary mechanism to avoid depressed suicides.

One discrepant finding was the lack of triage related, statistically significant difference in rBM in the lateral prefrontal cortices despite images showing areas of mildly reduced metabolism in dorsolateral frontal cortices visually. On CortexID software, the area used for quantification is very large compared to appreciably small areas. This may indicate dilution of the effect resulting in underestimation of rBM changes. Nonetheless, probably the fontal abnormality is not as severe in keeping with study by Huang et al. showing 14.2% gCBF decline in AD patients is associated with only 11.9% decline in frontal cortices (relative to occipital 21.3%).

Strengths of our study include a reasonable sample size, objective measurements of gBM and rBM with no inter-observer variations as well as manual relative metabolism. Brain measurements can suffer large ‘between’ (16.2%) and ‘within’ (4.8%) subject variabilities [25], former is eliminated in this study. A limitation

of the study is that we have inferred a physiological phenomenon in patients who had severe malignancy in the pre therapy PET and had just recovered with chemotherapy in post-therapy PET. However, the aim of the study was simply to observe regional changes if there is global hypometabolism rather than assessment of normal metabolism. Another limitation of this study is that we did not confirm that the decreased brain FDG activity was associated with reduced perfusion. We do recommend this should be further explored further in better designed studies.

Conclusion

A triage related metabolic redistribution has huge implications not only in understanding human behaviour during illness but also in explaining the well-known pathophysiological and epidemiological linkage between aging, delirium, SVD and AD. Our model has a strong emphasis on SVD as an umbrella pathology but dedicated designed studies are required to further elaborate on this. Linkage of cognition with intermittent illnesses in our model implies possible lower cognition in infection prevalent regions and further epidemiological studies are encouraged. Sex related difference in triage should be further explored for other non-neurodegenerative reversible neurological illnesses with high gender differences e.g. migraine and posterior reversible encephalopathy syndrome (PRES).

Disclosure of conflict of interest

None.

Address correspondence to: Sandeep K Gupta, Department of Nuclear Medicine & PET, John Hunter & Calvary Mater Hospitals, Newcastle, Australia. Tel: +61-249213390; Fax: +61-249213392; E-mail: Sandeep.Gupta@health.nsw.gov.au

References

[1] Fong TG, Vasunilashorn SM, Libermann T, Marcantonio ER and Inouye SK. Delirium and Alzheimer disease: a proposed model for shared pathophysiology. Int J Geriatr Psychiatry 2019; 34: 781-789.

[2] Jagust W. Imaging the evolution and pathophysiology of Alzheimer disease. Nat Rev Neurosci 2018; 19: 687-700.

[3] Fu H, Hardy J and Duff KE. Selective vulnerability in neurodegenerative diseases. Nat Neurosci 2018; 21: 1350-1358.

[4] Kato T, Inui Y, Nakamura A and Ito K. Brain fluorodeoxyglucose (FDG) PET in dementia. Ageing Res Rev 2016; 30: 73-84.

[5] Kawasaki K, Ishii K, Saito Y, Oda K, Kimura Y and Ishiwata K. Influence of mild hyperglycemia on cerebral FDG distribution patterns calculated by statistical parametric mapping. Ann Nucl Med 2008; 22: 191-200.

[6] Jack CR Jr, Wiste HJ, Weigand SD, Therneau TM, Lowe VJ and Knopman DS. Defining imaging biomarker cut points for brain aging and Alzheimer's disease. Alzheimer's Dement 2017; 13: 205-216.

[7] Liu PP, Xie Y, Meng XY and Kang JS. History and progress of hypotheses and clinical trials for Alzheimer's disease. Signal Transduct Target Ther 2019; 4: 29.

[8] Sweeney MD, Kisler K, Montagne A, Toga AW and Zlokovic BV. The role of brain vasculature in neurodegenerative disorders. Nat Neurosci 2018; 21: 1318-1331.

[9] Kealy J, Murray C, Griffin EW, Lopez-Rodriguez AB, Healy D, Tortorelli LS, Lowry JP, Watne LO and Cunningham C. Acute inflammation alters brain energy metabolism in mice and humans: role in suppressed spontaneous activity, impaired cognition, and delirium. J Neurosci 2020; 40: 5681-5696.

[10] Adams HJ, de Klerk JM, Fijnheer R, Heggelman BG, Dubois SV, Nievelstein RA and Kwee TC. Brain glucose metabolism in diffuse large B-cell lymphoma patients as assessed with FDG-PET: impact on outcome and chemotherapy effects. Acta radiol 2016; 57: 733-741.

[11] Nonokuma M, Kuwabara Y, Takano K, Tamura K, Ishitsuka K and Yoshimitsu K. Evaluation of regional cerebral glucose metabolism in patients with malignant lymphoma of the body using statistical image analysis. Ann Nucl Med 2014; 28: 950-960.

[12] Hanaoka K, Hosono M, Shimono T, Usami K, Komeya Y, Tsuchiya N, Yamazoe Y, Ishii K, Tatsumi Y and Sumita M. Decreased brain FDG uptake in patients with extensive non-Hodgkin's lymphoma lesions. Ann Nucl Med 2010; 24: 707-711.

[13] Sorokin J, Saboury B, Ahn JA, Moghbel M, Basu S and Alavi A. Adverse functional effects of chemotherapy on whole-brain metabolism. Clin Nucl Med 2014; 39: e35-39.

[14] Baudino B, D'Agata F, Caroppo P, Castellano G, Cauda S, Manfredi M, Geda E, Castelli L, Mortara P, Orsi L, Cauda F, Sacco K, Ardito RB, Pinessi L, Geminiani G, Torta R and Bisi G. The chemotherapy long-term effect on cognitive functions and brain metabolism in lymphoma

patients. Q J Nucl Med Mol Imaging 2012; 56: 559-568.
[15] Chiaravalloti A, Pagani M, Cantonetti M, Di Pietro B, Tavolozza M, Travascio L, DI Biagio D, Danieli R and Schillaci O. Brain metabolic changes in hodgkin disease patients following diagnosis and during the disease course: an 18F-FDG PET/CT study. Oncol Lett 2015; 9: 685-690.
[16] Manov JJ, Roth PJ and Kuker R. Clinical pearls: etiologies of superscan appearance on Fluorine-18-Fludeoxyglucose positron emission tomography-computed tomography. Indian J Nucl Med 2017; 32: 259-265.
[17] Simpson IA, Carruthers A and Vannucci SJ. Supply and demand in cerebral energy metabolism: the role of nutrient transporters. J Cereb Blood Flow Metab 2007; 27: 1766-1791.
[18] Sweeney MD, Sagare AP and Zlokovic BV. Blood-brain barrier breakdown in Alzheimer disease and other neurodegenerative disorders. Nat Rev Neuro 2018; 14: 133-150.
[19] Paulson OB, Hasselbalch SG, Rostrup E, Knudsen GM and Pelligrino D. Cerebral blood flow response to functional activation. J Cereb Blood Flow Metab 2010; 30: 2-14.
[20] Koehler RC, Roman RJ and Harder DR. Astrocytes and the regulation of cerebral blood flow. Trends Neurosci 2009; 32: 160-169.
[21] Cunnane SC, Trushina E, Morland C, Prigione A, Casadesus G, Andrews ZB, Beal MF, Bergersen LH, Brinton RD, de la Monte S, Eckert A, Harvey J, Jeggo R, Jhamandas JH, Kann O, la Cour CM, Martin WF, Mithieux G, Moreira PI, Murphy MP, Nave KA, Nuriel T, Oliet SHR, Saudou F, Mattson MP, Swerdlow RH and Millan MJ. Brain energy rescue: an emerging therapeutic concept for neurodegenerative disorders of ageing. Nat Rev Drug Discov 2020; 19: 609-633.
[22] Kisler K, Nelson AR, Montagne A and Zlokovic BV. Cerebral blood flow regulation and neurovascular dysfunction in Alzheimer disease. Nat Rev Neurosci 2017; 18: 419-434.
[23] Beuthien-baumann B, Handrick W, Schmidt T, Burchert W, Oehme L, Kropp J, Schackert G, Pinkert J and Franke WG. Persistent vegetative state: evaluation of brain metabolism and brain perfusion with pet and spect. Nucl Med Commun 2003; 24: 643-649.
[24] Stender J, Kupers R, Rodell A, Thibaut A, Chatelle C, Bruno MA, Gejl M, Bernard C, Hustinx R, Laureys S and Gjedde A. Quantitative rates of brain glucose metabolism distinguish minimally conscious from vegetative state patients. J Cereb Blood Flow Metab 2015; 35: 58-65.
[25] Clement P, Mutsaerts HJ, Václavů L, Ghariq E, Pizzini FB, Smits M, Acou M, Jovicich J, Vanninen R, Kononen M, Wiest R, Rostrup E, Bastos-Leite AJ, Larsson EM and Achten E. Variability of physiological brain perfusion in healthy subjects-a systematic review of modifiers. Considerations for multi-center ASL studies. J Cereb Blood Flow Metab 2018; 38: 1418-1437.
[26] Stoquart-ElSankari S, Balédent O, Gondry-Jouet C, Makki M, Godefroy O and Meyer ME. Aging effects on cerebral blood and cerebrospinal fluid flows. J Cereb Blood Flow Metab 2007; 27: 1563-1572.
[27] Zarrinkoob L, Ambarki K, Wåhlin A, Birgander R, Eklund A and Malm J. Blood flow distribution in cerebral arteries. J Cereb Blood Flow Metab 2015; 35: 648-654.
[28] Huang CW, Hsu SW, Chang YT, Huang SH, Huang YC, Lee CC, Chang WN, Lui CC, Chen NC and Chang CC. Cerebral perfusion insufficiency and relationships with cognitive deficits in Alzheimer's disease: a multiparametric neuroimaging study. Sci Rep 2018; 8: 1-14.
[29] Fong TG, Bogardus ST, Daftary A, Auerbach E, Blumenfeld H, Modur S, Leo-Summers L, Seibyl J and Inouye SK. Cerebral perfusion changes in older delirious patients using 99mTc HMPAO SPECT. J Gerontol A Biol Sci Med Sci 2006; 61: 1294-1299.
[30] Yokota H, Ogawa S, Kurokawa A and Yamamoto Y. Regional cerebral blood flow in delirium patients. Psy Clin Neurosci 2003; 57: 337-339.
[31] Haggstrom LR, Nelson JA, Wegner EA and Caplan GA. 2-18F-fluoro-2-deoxyglucose positron emission tomography in delirium. J Cereb Blood Flow Metab 2017; 37: 3556-3567.
[32] Yokota H, Ogawa S, Kurokawa A and Yamamoto Y. Regional cerebral blood flow in delirium patients. Psy Clin Neurosci 2003; 57: 337-339.
[33] Nitchingham A, Kumar V, Shenkin S, Ferguson KJ and Caplan GA. A systematic review of neuroimaging in delirium: predictors, correlates and consequences. Int J Geriatr Psychiatry 2018; 33: 1458-1478.
[34] Meng L, Hou W, Chui J, Han R and Gelb AW. Cardiac output and cerebral blood flow. Anesthesiology 2015; 123: 1198-1208.
[35] Ogawa K, Uema T, Motohashi N, Nishikawa M, Takano H, Hiroki M, Imabayashi E, Ohnishi T, Inoue T, Takayama Y, Takeda M, Matsuda H, Andoh T and Yamada Y. Neural mechanism of propofol anesthesia in severe depression: a positron emission tomographic study. Anesthesiology 2003; 98: 1101-1111.
[36] Vandesteene A, Trempont V, Engelman E, Deloof T, Focroul M, Schoutens A and de Rood M. Effect of propofol on cerebral blood flow and metabolism in man. Anaesthesia 1988; 43: 42-43.

[37] Forster A, Juge O and Morel D. Effects of midazolam on cerebral blood flow in human volunteers. Anesthesiology 1982; 56: 453-455.
[38] Ghaznawi R, Zwartbol MH, Zuithoff NP, Bresser J, Hendrikse J and Geerlings MI; UCC-SMART Study Group. Reduced parenchymal cerebral blood flow is associated with greater progression of brain atrophy: the SMART-MR study. J Cereb Blood Flow Metab 2020; 41: 1229-1239.
[39] Roher AE, Debbins JP, Malek-Ahmadi M, Chen K, Pipe JG, Maze S, Belden C, Maarouf CL, Thiyyagura P, Mo H, Hunter JM, Kokjohn TA, Walker DG, Kruchowsky JC, Belohlavek M, Sabbagh MN and Beach TG. Cerebral blood flow in Alzheimer's disease. Vasc Health Risk Manag 2012; 8: 599-611.
[40] Erdö F, Denes L and de Lange E. Age-associated physiological and pathological changes at the blood-brain barrier: a review. J Cereb Blood Flow Metab 2017; 37: 4-24.
[41] Busche MA and Hyman BT. Synergy between amyloid-β and tau in Alzheimer's disease. Nat Neurosci 2020; 23: 1183-1193.
[42] Wardlaw JM, Benveniste H, Nedergaard M, Zlokovic BV, Mestre H, Lee H, Doubal FN, Brown R, Ramirez J, MacIntosh BJ, Tannenbaum A, Ballerini L, Rungta RL, Boido D, Sweeney M, Montagne A, Charpak S, Joutel A, Smith KJ and Black SE; colleagues from the Fondation Leducq Transatlantic Network of Excellence on the Role of the Perivascular Space in Cerebral Small Vessel Disease. Perivascular spaces in the brain: anatomy, physiology and pathology. Nat Rev Neurol 2020; 16: 137-153.
[43] Iturria-Medina Y, Sotero RC, Toussaint PJ, Mateos-Pérez JM and Evans AC; Alzheimer's Disease Neuroimaging Initiative. Early role of vascular dysregulation on late-onset Alzheimer's disease based on multifactorial data-driven analysis. Nat Commun 2016; 7: 11934.
[44] Subramaniyan S and Terrando N. Neuroinflammation and perioperative neurocognitive disorders. Anesth Analg 2019; 128: 781-788.
[45] Kalvas LB and Monroe TB. Structural brain changes in delirium: an integrative review. Biol Res Nurs 2019; 21: 355-365.
[46] Vestergaard MB, Jensen ML, Arngrim N, Lindberg U and Larsson HB. Higher physiological vulnerability to hypoxic exposure with advancing age in the human brain. J Cereb Blood Flow Metab 2020; 40: 341-353.
[47] Jackson JC, Hopkins RO, Miller RR, Gordon SM, Wheeler AP and Ely EW. Acute respiratory distress syndrome, sepsis, and cognitive decline: a review and case study. South Med J 2009; 133: 181-190.
[48] Joo IL, Lai AY, Bazzigaluppi P, Koletar MM, Dorr A, Brown ME, Thomason LA, Sled JG, McLaurin J and Stefanovic B. Early neurovascular dysfunction in a transgenic rat model of Alzheimer's disease. Sci Rep 2017; 7: 1-14.
[49] Heeman F, Yaqub M, Alves IL, Heurling K, Bullich S, Gispert JD, Boellaard R and Lammertsma AA; AMYPAD Consortium. Simulating the effect of cerebral blood flow changes on regional quantification of [18F]flutemetamol and [18F]florbetaben studies. J Cereb Blood Flow Metab 2021; 41: 579-589.
[50] Semmler A, Hermann S, Mormann F, Weberpals M, Paxian SA, Okulla T, Schäfers M, Kummer MP, Klockgether T and Heneka MT. Sepsis causes neuroinflammation and concomitant decrease of cerebral metabolism. J Neuroinflammation 2008; 5: 38.
[51] Takkinen JS, López-Picón FR, Al Majidi R, Eskola O, Krzyczmonik A, Keller T, Löyttyniemi E, Solin O, Rinne JO and Haaparanta-Solin M. Brain energy metabolism and neuroinflammation in ageing APP/PS1-21 mice using longitudinal 18F-FDG and 18F-DPA-714 PET imaging. J Cereb Blood Flow Metab 2017; 37: 2870-2882.
[52] Ishibashi K, Onishi A, Fujiwara Y, Oda K, Ishiwata K and Ishii K. Longitudinal effects of aging on 18F-FDG distribution in cognitively normal elderly individuals. Sci Rep 2018; 8: 11557.
[53] Moeini M, Lu X, Avti PK, Damseh R, Bélanger S, Picard F, Boas D, Kakkar A and Lesage F. Compromised microvascular oxygen delivery increases brain tissue vulnerability with age. Sci Rep 2018; 8: 8219.
[54] Zlokovic BV. Neurovascular pathways to neurodegeneration in Alzheimer's disease and other disorders. Nat Rev Neurosci 2011; 12: 723-738.
[55] Hall CN, Reynell C, Gesslein B, Hamilton NB, Mishra A, Sutherland BA, O'Farrell FM, Buchan AM, Lauritzen M and Attwell D. Capillary pericytes regulate cerebral blood flow in health and disease. Nature 2014; 508: 55-60.
[56] Van Dijk EJ, Prins ND, Vermeer SE, Vrooman HA, Hofman A, Koudstaal PJ and Breteler MM. C-reactive protein and cerebral small-vessel disease: the Rotterdam scan study. Circulation 2005; 112: 900-905.
[57] Di X, Wölfer M, Amend M, Wehrl H, Ionescu TM, Pichler BJ and Biswal BB; Alzheimer's Disease Neuroimaging Initiative. Interregional causal influences of brain metabolic activity reveal the spread of aging effects during normal aging. Hum Brain Mapp 2019; 40: 4657-4668.
[58] Shafi MM, Santarnecchi E, Fong TG, Jones RN, Marcantonio ER, Pascual-Leone A and Inouye SK. Advancing the neurophysiological understanding of delirium. J Am Geriatr Soc 2017; 65: 1114-1118.
[59] Wang J, Gu BJ, Masters CL and Wang YJ. A systemic view of Alzheimer disease-insights from

amyloid-β metabolism beyond the brain. Nat Rev Neurol 2017;13: 612-623.
[60] Dantzer R. Cytokine-induced sickness behaviour: a neuroimmune response to activation of innate immunity. Eur J Pharmacol 2004; 500: 399-411.
[61] Østergaard L, Engedal TS, Moreton F, Hansen MB, Wardlaw JM, Dalkara T, Markus HS and Muir KW. Cerebral small vessel disease: capillary pathways to stroke and cognitive decline. J Cereb Blood Flow Metab 2016; 36: 302-325.
[62] Ter Telgte A, Van Leijsen EMC, Wiegertjes K, Klijn CJM, Tuladhar AM and De Leeuw FE. From a focal to a global perspective. Nat Rev Neurol 2018; 14: 387-398.
[63] Tarasoff-Conway JM, Carare RO, Osorio RS, Glodzik L, Butler T, Fieremans E, Axel L, Rusinek H, Nicholson C, Zlokovic BV, Frangione B, Blennow K, Ménard J, Zetterberg H, Wisniewski T and de Leon MJ. Clearance systems in the brain-implications for Alzheimer disease. Nat Rev Neurol 2015; 11: 457-470.
[64] Counts SE, Ikonomovic MD, Mercado N, Vega IE and Mufson EJ. Biomarkers for the early detection and progression of Alzheimer's disease. Neurotherapeutics 2017; 14: 35-53.
[65] Kotliar K, Hauser C, Ortner M, Muggenthaler C, Diehl-Schmid J, Angermann S, Hapfelmeier A, Schmaderer C and Grimmer T. Altered neurovascular coupling as measured by optical imaging: a biomarker for Alzheimer's disease. Sci Rep 2017; 7: 12906.
[66] Masters CL, Bateman R, Blennow K, Rowe CC, Sperling RA and Cummings JL. Alzheimer's disease. Nat Rev Dis Prim 2015; 1: 15056.
[67] Greenberg SM, Bacskai BJ, Hernandez-Guillamon M, Pruzin J, Sperling R and van Veluw SJ. Cerebral amyloid angiopathy and Alzheimer disease-one peptide, two pathways. Nat Rev Neurol 2020; 16: 30-42.
[68] Leuzy A, Chiotis K, Lemoine L, Gillberg PG, Almkvist O, Rodriguez-Vieitez E and Nordberg A. Tau PET imaging in neurodegenerative tauopathies-still a challenge. Mol Psychiatry 2019; 24: 1112-1134.
[69] Franzmeier N, Neitzel J, Rubinski A, Smith R, Strandberg O, Ossenkoppele R, Hansson O and Ewers M; Alzheimer's Disease Neuroimaging Initiative (ADNI). Functional brain architecture is associated with the rate of tau accumulation in Alzheimer's disease. Nat Commun 2020; 11: 347.
[70] Villemagne VL, Doré V, Burnham SC, Masters CL and Rowe CC. Imaging tau and amyloid-β proteinopathies in Alzheimer disease and other conditions. Nat Rev Neurol 2018; 14: 225-236.
[71] Meles SK, Pagani M, Arnaldi D, De Carli F, Dessi B, Morbelli S, Sambuceti G, Jonsson C, Leenders KL and Nobili F. The Alzheimer's disease metabolic brain pattern in mild cognitive impairment. J Cereb Blood Flow Metab 2017; 37: 3643-3648.
[72] Aanerud J, Borghammer P, Rodell A, Jónsdottir KY and Gjedde A. Sex differences of human cortical blood flow and energy metabolism. J Cereb Blood Flow Metab 2017; 37: 2433-2440.
[73] Launer LJ, Andersen K, Dewey ME, Letenneur L, Ott A, Amaducci LA, Brayne C, Copeland JR, Dartigues JF, Kragh-Sorensen P, Lobo A, Martinez-Lage JM, Stijnen T and Hofman A. Rates and risk factors for dementia and Alzheimer's disease: results from EURODEM pooled analyses. EURODEM Incidence Research Group and Work Groups. European Studies of Dementia. Neurology 1999; 52: 78-84.
[74] Alzheimer Association. Alzheimer's Disease facts and figures 2019. Alzheimer's Dement 2019.
[75] Chiotis K, Savitcheva I, Poulakis K, Saint-Aubert L, Wall A, Antoni G and Nordberg A. [18F] THK5317 imaging as a tool for predicting prospective cognitive decline in Alzheimer's disease. Mol Psychiatry 2020; [Epub ahead of print].
[76] Strange BA and Dolan RJ. Anterior medial temporal lobe in human cognition: memory for fear and the unexpected. Cogn Neuropsychiatry 2006; 11: 198-218.
[77] Touroutoglou A, Andreano J, Dickerson BC and Barrett LF. The tenacious brain: how the anterior mid-cingulate contributes to achieving goals. Cortex 2020; 123: 12-29.
[78] Moriguchi S, Takamiya A, Noda Y, Horita N, Wada M, Tsugawa S, Plitman E, Sano Y, Tarumi R, ElSalhy M, Katayama N, Ogyu K, Miyazaki T, Kishimoto T, Graff-Guerrero A, Meyer JH, Blumberger DM, Daskalakis ZJ, Mimura M and Nakajima S. Glutamatergic neurometabolite levels in major depressive disorder: a systematic review and meta-analysis of proton magnetic resonance spectroscopy studies. Mol Psychiatry 2019; 24: 952-964.
[79] Lichenstein SD, Verstynen T and Forbes EE. Adolescent brain development and depression: a case for the importance of connectivity of the anterior cingulate cortex. Neurosci Biobehav Rev 2016; 70: 271-287.
[80] Tanti A, Lutz PE, Kim J, O'Leary L, Théroux JF, Turecki G and Mechawar N. Evidence of decreased gap junction coupling between astrocytes and oligodendrocytes in the anterior cingulate cortex of depressed suicides. Neuropsychopharmacology 2019; 44: 2099-2111.